Constraints on crustal recycling from boron isotopes in Italian melt inclusions

Earth Planet. Sci. Lett. 624 (2023) 118462

Contents lists available at ScienceDirect

Earth and Planetary Science Letters

journal homepage: www.elsevier.com/locate/epsl

Constraints on crustal recycling from boron isotopes in Italian melt inclusions

Natascia Luciani [a,*], Igor K. Nikogosian [a], Cees-Jan De Hoog [b], Gareth R. Davies [a], Janne M. Koornneef [a]

[a] Vrije Universiteit Amsterdam, the Netherlands
[b] The University of Edinburgh, United Kingdom

ARTICLE INFO

Keywords:
Melt inclusions
Boron isotopes
Italian magmatism
Post-collisional volcanism

ABSTRACT

Boron represents an important tracer of crustal recycling processes in subduction zones, because it is readily mobilised from the subducted lithosphere and different components in the slab are isotopically distinct. Profiles of boron content and isotope ratio across magmatic arcs generally show that B concentrations decrease with increasing slab depth, which implies decreasing amount of slab-derived fluids. To date, however, data on continental-collision zones and post-collisional subduction settings are scarce.

This study examines Plio-Quaternary Italian magmatism to quantify crustal recycling in a complex subduction setting. Magmatic products vary from (ultra)potassic along the Tyrrhenian side in the north, to calcalkaline and Na-alkaline in the south.

Combined major and trace element and [B] content and $\delta^{11}B$ values are reported in 99 Melt Inclusions (MIs), analyses from a wide range of Italian lavas. [B] vary from 4 to 298 μg/g and $\delta^{11}B$ from -29.2 to -3.9‰. The B isotopic values are considerably lower than previously reported in arcs and other post-collisional setting magmatism. We infer a role for phengite in the source of all studied Italian magmas (with the exception of Mt. Etna lavas). This white mica is stable to high pressures in subducted sediments of altered oceanic crust and records dehydration and ^{11}B depletion due to dehydration processes.

MIs hosted in highly fosteritic olivines (Fo >74; median of 89) from across Italy reveal that primary melts tap heterogeneous mantle including subducted oceanic and continental components that were introduced during the Alpine, and Adriatic and Ionian subduction phases.

The combined geochemical data record the involvement of sediments that variably metasomatized the mantle wedge. We propose that slab detachment and consequent heat input from the inflow of hot asthenosphere was responsible for phengite breakdown in subducted sediments and locally produced metasomatism of the mantle wedge, imposing a characteristic B isotope signature to the overlying mantle. Continued heating due to asthenosphere inflow led to melting of the metasomatized mantle wedge and generation of the Italian magmatism. Mt. Etna represents an exception being dominated by asthenosphere upwelling through a slab window with minimal influence from active subduction.

1. Introduction

Boron (B) with its stable isotopes ^{10}B and ^{11}B is a potential tracer of recycled crustal material in the mantle because of isotopic fractionation at low temperatures and its incompatible fluid-mobile behaviour during melting (Palmer et al., 1996; Marschall et al., 2017; De Hoog and Savov, 2018). Boron concentration and isotope compositions have been reported for many subduction zone lavas (e.g., Ishikawa and Nakamura, 1994; Tonarini et al., 2011; Iveson et al., 2021) however, data on continental-collision zones and post-collisional subduction settings are limited and the focus of this work.

B isotopes are predicted to be a sensitive indicator of recycling in subduction zones because the incompatibility of B leads to a low concentration in the mantle (mid-ocean ridge basalts (MORBs; <1 μg/g) with a homogeneous $\delta^{11}B$ value of −7.1 ± 0.9 ‰ (Marschall et al., 2017). When MORBs interacts with seawater at low temperature (<100

* Corresponding author.
E-mail address: n.luciani@vu.nl (N. Luciani).

https://doi.org/10.1016/j.epsl.2023.118462
Received 12 December 2022; Received in revised form 17 October 2023; Accepted 22 October 2023
Available online 4 November 2023

ºC), B is incorporated in secondary minerals (e.g., clay minerals), and isotopically fractionated (i.e.; Berndt and Seyfried, 1990; Smith et al., 1995) resulting in large variability in B concentration and isotope ratio in altered oceanic crust (AOC); ([B]=10–90 μg/g; δ^{11}B from 0 to +18‰; Marschall, 2018). Boron and the heavy isotope ^{11}B are strongly enriched in marine-, ([B] from 1 to >100 μg/g; δ^{11}B from +2 to +26‰) and continental-sediments ([B]=50–150 μg/g; δ^{11}B from +13 to +8‰; De Hoog and Savov, 2018). Seawater has a higher δ^{11}B value (+39.6‰; Foster et al., 2010). The major B reservoirs in sediments are clays (~ 100 μg/g; Ishikawa and Nakamura 1993; Palmer et al., 1996), micas ([B] up to 2000 μg/g; e.g., Harder 1970; Leeman and Sisson, 2018), and tourmaline ([B] up to 33,000 μg/g; e.g., Marschall et al., 2006). Fractionation of boron isotopes during incorporation onto clays yields typical δ^{11}B values of ~+15‰ (Palmer, 2017, and reference therein). In contrast, phengite (metamorphic white mica) has been reported in the literature with δ^{11}B as low as −29‰ (Halama et al., 2014; Menold et al., 2016), and this phase is stable to depths of arc magma genesis (Klemme et al., 2011). With [B] up to 500 μg/g, if present this phase is liable to dominate the boron budget of the solid phases in the subducting lithosphere (Marschall et al., 2006; Guo et al., 2022).

Small B additions from surface materials to the depleted mantle can be detected because of the marked contrast in concentration and isotopic composition between the two reservoirs. B isotopic fractionation during progressive dehydration of the subducting lithosphere (slab) liberates ^{11}B-rich fluids (e.g., Rosner et al., 2003; Konrad-Schmolke and Halama, 2014). Isotopic variation in the slab is thought to occur due to a combination of physical parameters influencing the sediment transfer and boron dehydration and fractionation processes, such as steepness of the slab and depth of the slab and trench-arc front distance (De Hoog and Savov, 2018). Generally, magmatism records across-arc variation with a decrease of [B] and δ^{11}B with increasing slab depth (Ishikawa and Nakamura, 1994).

Here we present combined major and trace element and [B] and δ^{11}B compositions of primary melt inclusions (MIs) preserved in high-Fo olivine phenocrysts (Fo% 74–94) from potassic and ultrapotassic volcanic rocks from across the Italian Peninsula and Mt. Etna. MIs are pockets of magma (10–100 μm in diameter) trapped in minerals such as olivine that grow at mantle depths (e.g., Kamenetsky et al., 2002; Kent, 2008). After entrapment in the mineral, MIs are unaffected by processes such as magma mixing and crustal contamination that occur within the crust. Few studies report boron compositions in Italian olivine-hosted MIs despite boron representing a strong tool for fingerprinting recycled sediments and fluids in complex subduction zones (Palmer et al., 2019; Sugden et al., 2020; Tonarini et al., 2001). This paper aims to better understand sediment recycling and transfer mechanisms to account for marked compositional variability in this complex collisional setting.

2. Geological setting and samples

The volcanic activity in Italy is the result of the convergence of Africa and the Eurasian plate, related to the Cretaceous-Oligocene south- to eastward Alpine subduction in the north of the peninsula, to the southwest to westward subduction of Adriatic continental lithosphere in the centre, and the Ionian oceanic lithosphere subduction in the south (Miocene to recent; Carminati and Doglioni, 2012, and reference therein). Today, subduction of the Adriatic plate has ceased, however, in the Calabrian/Ionian, subduction and volcanism is still active. Evidence of southeast-ward rollback of the southern part of the Ionian plate is recorded in tomographic images and earthquakes (e.g., Schellart, 2010). Furthermore, a tear propagating from the northern to the southern magmatic provinces is confirmed by available tomographic images of the Apennine subduction zone, and numerical model calculations and surface uplift support the presence of a slab detachment propagating along the Apennines (e.g., Spakman and Wortel, 2004).

During the Apennine stage, a diverse range of magmatic compositions were formed, mafic to felsic and from subalkaline to ultra-alkaline magmatic compositions, was observed. Notably, in the Plio-Quaternary era, significant magmatic events occurred in central-southern Italy, exhibiting abundant ultrapotassic magmatism. Numerous studies have concluded that this compositional variability is indicative of magmas originating from a highly heterogeneous and anomalous upper mantle (e.g., Peccerillo, 1999; D'Antonio et al., 1999; Conticelli et al., 2002; Nikogosian and van Bergen, 2010, Koornneef et al., 2019). The mantle composition results from the continuous input of diverse crustal materials and the upwelling of asthenosphere or deep mantle rocks in specific regions (e.g., Peccerillo, 2005; Peccerillo and Frezzotti, 2015).

Incompatible trace element distributions and isotopic compositions of these magmas closely resemble those of upper crustal rocks (Rudnick and Fountain, 1995; Conticelli et al., 2009). These characteristics strongly suggest significant recycling of subducted sediments. Numerous studies support the hypothesis that the ultrapotassic and potassic Italian magmatism derives from a peridotitic mantle metasomatized by subduction-derived fluids/melts that produced a vein network rich in K-bearing phases (phlogopite±amphibole; e.g., Conticelli et al., 2015; Peccerillo and Frezzotti, 2015).

A characteristic of Italian ultrapotassic rocks is their close temporal and spatial association with shoshonitic rocks and high-K calc-alkaline suites. The transition from the high-K series (HKS) to shoshonitic (SHO) and high K-Ca series (HKCA) in the Roman province, for example, has been attributed to an increase in melting degrees within a veined and metasomatized mantle, where the veins contribute to magmas with higher crustal enrichment (e.g., kamafugites-KAM, and HKS; Avanzinelli et al., 2009; Conticelli et al., 2009). In their models greater melting leads to dilution of the vein signature, resulting in less enriched SHO and HKCA magmas. The inflow of asthenosphere material was proposed as a possible factor contributing to the increased melting degrees (Conticelli et al., 2009; Avanzinelli et al., 2009).

In contrast, investigations focusing on major and trace-element systematics in olivine-hosted melt inclusions (MIs) in Pliocene– Quaternary potassic volcanic Italian rocks (e.g., Nikogosian and van Bergen, 2010; Schiavi et al., 2012; Koornneef et al., 2015; 2019; Nikogosian et al., 2016) established that the different magmatic series originated from separate sources within a heterogeneous vein-type mantle lithologies formed by subduction recycling.

The Miocene to Quaternary potassic and ultrapotassic suites along the Tyrrhenian border of peninsular Italy, can be divided into different compositional provinces, where magmatism is confined in terms of space, time and petrographic characteristics. The age of the volcanic products decreases from Tuscany (8 Ma) towards the south of Italy, where the volcanism is still active (Peccerillo, 2017, and reference therein). In order to provide an overview of the tectono-magmatic processes responsible for the magmatism, we analysed MIs trapped in the most primitive olivine (Fo >74; median of 89) from the Quaternary-Pliocene lavas from 10 different volcanoes from six distinct Italian volcanic provinces (Fig.1):

1) Intra-Apennine province comprises a monogenetic volcano San Venanzo that erupted mafic products (0.6–0.4 Ma; Rosatelli et al., 2010). We analysed the Pian di Celle kamafugite lava flow (Nikogosian et al., 2019).
2) Tuscan province is characterised by the emplacement of leucite-free high-K to shoshonite (SHO) and calc-alkaline (CA) magmatic products. The most recent (Plio-Quaternary) intrusive and eruptive products from this area range from basic to lamproites. In this paper, we report data from Torre Alfina lamproites.
3) Roman province characterised by leucite-bearing high-K serie (HKS) rocks and younger SHO to CA products (~0.8–0.02 Ma; e.g., Peccerillo, 2017, and reference therein; Frezzotti et al., 2007). Here we selected HKS lavas from Vulsini, Sabatini, Alban Hills volcanoes and

Fig. 1. Sketch map of the Italian peninsula showing distribution of Plio-Quaternary magmatic provinces.

SHO from Latera volcano in the Vulsini district (Selva del Lamone lava flow; Nikogosian et al., 2016).

4) Ernici-Roccamonfina province is characterised by sub alkaline to ultrapotassic rocks (0.7–0.1 Ma). The ultrapotassic rocks are similar to the Roman province, where the calc-alkaline to potassic rocks are similar to the Campanian volcanic province below. For the current study, we selected representative samples for Roccamonfina HKCA-SHO—HKS and Ernici HKS-CA series (Nikogosian and van Bergen, 2010; Koornneef et al., 2015, 2019).
5) Campanian province (Phlegrean Fields and Mt. Vesuvius) products are classified as potassic and HKS, however, rare calc-alkaline basalts are present as xenoliths and lavas in the Pontine archipelago (Peccerillo, 2017, and references therein). We report data from the 1834 C.E. Mt. Vesuvius eruption and Accademia deposit lava samples from Phlegrean Fields.
6) Mt. Etna (~0.6 Ma to present) generated products with tholeiitic compositions, followed by more recent sodic to potassic alkaline compositions. We selected potassic alkaline lava samples from the Mongibello stage of 1669 C.E. eruption.

3. Methods

Lava samples were crushed and sieved to separate the olivine phenocrysts. Phenocrysts were embedded in epoxy and polished on one side for electron microprobe analysis (EMPA). The olivine grains with the highest forsterite content (Fo) hosting MIs were selected for experimental and analytical study to determine melt compositions. About 200 experiments were performed to re-homogenize and quench MIs to glass using a high-T heating/quenching stage at the Vrije Universiteit Amsterdam, according to experimental procedures described in Nikogosian and van Bergen (2010). The homogenised host-olivine grains were then polished until the MIs were exposed at the surface for major, trace, and volatile element analysis.

Concentrations of major elements and volatiles in host olivine and MIs were obtained by EMPA using a JEOL JXA8600 at Utrecht University, largely following methods and techniques described by De Hoog et al. (2001). Natural minerals, metals and synthetic oxide were used as reference materials. Concentrations of trace elements in the quenched MIs were determined by secondary ion mass spectrometry (SIMS) using a CAMECA IMS4f at the Institute of Microelectronics (Yaroslavl', Russia) and by laser ablation inductively coupled plasma mass spectrometry (LA-ICP-MS) using a GeoLas 200Q Excimer laser ablation system (193 nm wavelength) coupled with a Thermo Finnigan Element 2 sector field ICP-MS instrument at Utrecht University following the techniques of Mason et al. (2008).

MI compositions were corrected for the post-entrapment "Fe-loss" process using the method described by Danyushevsky et al. (2000) combined with "Petrolog3" integrated software (Danyushevsky and Plechov, 2011). For the correction, we assumed that the initial FeO content corresponded to the FeO content of the host rocks. In the procedure, we applied the olivine-melt equilibrium model of Ford et al. (1983) using Fe^{2+}/Fe^{3+} ratios in the melt as estimated in coexisting olivine-hosted Cr-spinel inclusions and the spinel-melt equilibria of Maurel and Maurel (1982). The correction procedure affects MgO and FeO content with insignificant impact on other major element oxides.

Boron contents and $\delta^{11}B$ ratios of the MIs were measured by SIMS using a Cameca IMS 7f-Geo ion microprobe at the Edinburgh Ion Microprobe Facility, following the setup detailed in Wu et al. (2021).

Boron isotope compositions are expressed in $\delta^{11}B$ ($\delta^{11}B = \{[(^{11}B/^{10}B_{sample})/(^{11}B/^{10}B_{NIST\text{-}SRM951}) - 1]$

4. Results

Major and trace element compositions for the MIs and host rocks are presented in Tables S.1; Figs. 2 and 3 and Fig. S1. Boron concentrations and boron isotope compositions of 99 MIs are presented in Table S.2 and Fig. 4.

The studied lavas represent relatively unevolved magmas (MgO > 4 wt.%) from different Italian provinces and magmatic series that carry olivine as a liquidus phase. Mafic Pliocene–Quaternary volcanic rocks of Italy are classified according to their K_2O/Na_2O ratio and degree of silica saturation (Peccerillo, 2017). Collectively, our studied samples cover the entire

Italian spectrum from Si-undersaturated to Si-oversaturated, from CA, HKCA and SHO to HKS compositions (Fig. 2). The studied host olivine (Fig. S.2) range between Fo 93 and Fo 83 mol.%, but all series have olivine with high-Fo (> 88 mol.%) and they represent parental or primary mantle-derived melts. Mt. Etna is the exception with low Fo 76–74 mol.% olivine.

4.1. Major and trace elements

Olivine-hosted MIs appear mostly as isolated inclusions with a diameter between 20 and 150 μm with a sub-spherical shape. Compositions of homogenized and corrected MIs are shown in Table S.1, S.3; Figs. 2 and 3.

MIs of Tuscan lamproites (Fo_{93-89}, MgO 6–12 wt.%) are characterized by the highest K_2O (10.7–14.5 wt.%), SiO_2 (48–60.5 wt.%), F (3000–6000 μg/g), and La/Yb (>35) contents and they have the widest range of Ce (74–463 μg/g). the Tuscan lamproites contain the lowest CaO (< 5 wt.%), Al_2O_3 (< 11 wt.%), Na_2O (< 1 wt.%), Cl (< 170 μg/g) and S (< 1100 μg/g) contents. Compared to other high-K Italian MIs, San Venanzo kamafugite melts ($Fo_{91-92.5}$, MgO 7–11 wt.%) have lower SiO_2 (40–43.5 wt.%), Al_2O_3 (10.5–12.5 wt.%) and higher TiO_2 (1–2 wt.%), CaO (>16 wt.%), P_2O_5 (0.5–1.2 wt.%), F (6000–8000 μg/g), S (3000–6000 μg/g) content. The main differences between SHO (Fo_{86-90}, MgO 6–11 wt.%) and HKS ($Fo_{84-91.6}$, MgO 5–11 wt.%) MIs within the

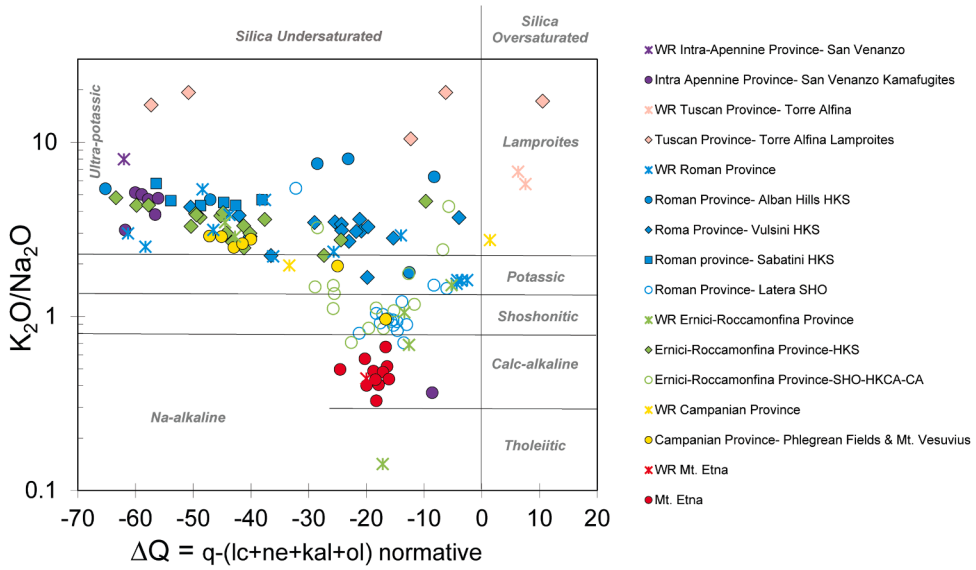

Fig. 2. Classification diagram of Italian MIs and respective host mafic rocks (WR; MgO > 4.0 wt.%) from this study based on K_2O/Na_2O (wt.%) ratio and degree of silica saturation. ΔQ is the algebraic sum of normative quartz (q) minus undersaturated minerals (leucite-lc, (nepheline-ne, kalsilite-kal, olivine-ol). Rocks with ΔQ ⟨ 0 are undersaturated in silica whereas rocks with ΔQ ⟩ 0 are silica oversaturated.

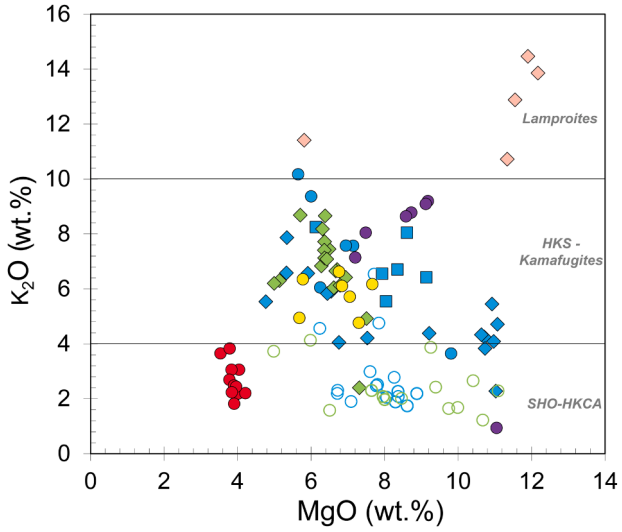

Fig. 3. K_2O (wt.%) vs MgO (wt.%) content for the Italian MIs reported in this study. MIs with K_2O > 10 (wt.%) are classified as lamproites; MIs with K_2O between 4 and 10 (wt.%) are classified as HKS Kamafugites; MIs with K_2O < 4 (wt.%) are classified as SHO—HKCA series. Symbols as in Fig.2.

Roman and Ernici-Roccamonfina provinces is the lower K_2O (1.2 - 4.5 vs 4 - 8.5 wt.%), P_2O_5 (< 0.3 vs > 0.3 wt.%), F (<1200 vs > 1000 μg/g) La/Yb (<20 vs >20) and higher Na_2O (> 1.7 vs < 1.7 wt.%) higher SiO_2 (45–50 vs 42–45 wt.%) for the Roman province. The Ce range is lower (between 57 and 83 μg/g) for SHO samples compared to the HKS samples (between 97 and 291 μg/g), with the exception of one outlier for Latera SHO (398.1 μg/g).

A comparison between the MIs with SHO composition from Latera (Roman province) and Ernici-Roccamonfina, show that the former contains higher CaO (15–17 vs 10–15 wt.%), S (3000–8000 vs 1000–5000 μg/g), Cl (500–1800 vs < 300 μg/g), Ba/La (> 20 vs < 15) and Ba/Th (> 100 vs < 30) and lower Na_2O (<1.8 vs > 2 wt.%), and Th/Nb (1–2.4 vs 0.6–1.4). Mt. Vesuvius HKS melts ($Fo_{87–90.2}$, MgO 5.8–7.7 wt.%) are distinct from all other Italian melts by the high Cl content (5000–6500 μg/g vs < 1700 μg/g). Evolved Mt. Etna melts ($Fo_{74–76}$, MgO 3.5–4.2 wt.%) are characterized by relatively high Al_2O_3 (17–19 wt.%), Na_2O (5 – 6.4 wt.%), Cl (2000–4000 μg/g), La/Yb (> 30) and low S (50–3000 μg/g), F (500–1350 μg/g) and Th/Nb (< 0.17).

4.2. Boron concentration and isotope composition

Italian MIs cover a wide range of [B] (4–298 μg/g) and $\delta^{11}B$ values (−29.2 to −3.9‰; Fig. 4; Table S.2). The [B] for San Venanzo, Torre Alfina, Roman province and Ernici-Roccamonfina HKS are in the range typical of continental crust, continental sediments and metasediments, higher than MORB, AOC and arc volcanics (see Fig.4). Ernici-Roccamonfina SHO and Mt. Etna have lower [B], comparable to MORB and AOC. These concentrations are typical of arcs, including published whole rock and olivine-hosted MIs data from Stromboli (Fig. 4).

There appears to be no correlation between the boron content and isotope composition of the Italian samples (Fig. 4). However, in general, there is an increase of $\delta^{11}B$ in MIs values from the northern to the southern volcanic provinces (see table S.2 and Fig. 5 from more details). San Venanzo MIs have the lowest $\delta^{11}B$ values, −29.2 to −24.5‰, with high [B], between 200 and 260 μg/g ($n = 7$; 1SD= ±0.5‰). Torre Alfina MIs cover a large range of [B] from 18 to 263 μg/g, as well as highly variable $\delta^{11}B$ values, −22.1 to −4.2‰ ($n = 7$; 1SD= ±1.0‰).

The Roman province MIs (Alban Hills, Latera, Sabatini, and Vulsini volcanoes) exhibit a consistent average boron (B) isotope ratio but display a wide range of [B]. SHO and HKS compositions are distinct within the Roman and Ernici-Roccamonfina provinces. The HKS MIs exhibit more negative $\delta^{11}B$ values and higher [B] compared to the SHO MIs. Similar B concentrations in MIs containing high-Forsterite (Fo) olivine were reported in the Vulsini volcano from the Roman province ([B]=61–100 μg/g) by Metrich et al. (1998).

The $\delta^{11}B$ values, in conjunction with B concentrations, generally decrease towards the southern provinces, such as the Campanian Province (Vesuvius and Phlegraean Fields). Tonarini et al. (2004) analysed $\delta^{11}B$ values and [B] in bulk basaltic to phonolitic rocks from the Phlegrean Fields. Their results have slightly more positive isotopic ratios (−8 to −3.3‰) and lower [B] (7 to 11 μg/g) compared to the findings of this study ($\delta^{11}B$ from −20.2 to −11.5‰ and [B] from 19 to 150 μg/g). Mt. Etna, has less negative $\delta^{11}B$ values compared to all other samples studied ($\delta^{11}B$ from −14.2 to −4.5‰) and together with Ernici-Roccamonfina SHO the lower [B] range (11–18 μg/g for Mt. Etna

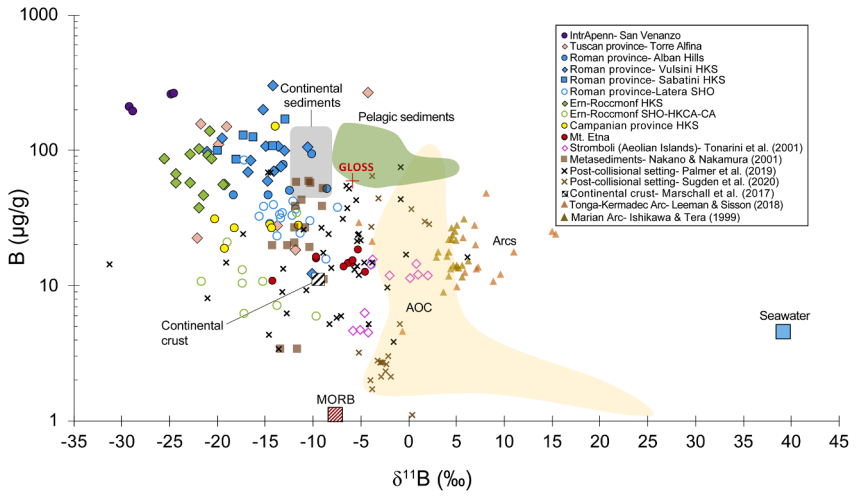

Fig. 4. B (µg/g) vs. δ^{11}B (‰) data for Italian MIs, including Schiavi et al. (2012) and data from Stromboli volcano (Aeolian islands) and whole rocks from Tonarini et al. (2001). For comparison [B] and isotope compositions of various reservoirs: continental sediments (De Hoog and Savov, 2018); continental crust and MORB (mid ocean ridge basalts; Marschall et al., 2017); AOC (altered oceanic crust; yellow field; Smith et al., 1995); seawater (Foster et al., 2010); metasediments (Nakano and Nakamura, 2001) and pelagic sediments (green field; Ishikawa and Nakamura, 1993). GLOSS (red cross; Plank, 2014). Data on whole rock for typical arc settings: Mariana arc (Ishikawa and Tera, 1999) and Tonga-Kermadec arc (Leeman and Sisson, 2018). Whole rock data from post-collisional settings by Palmer et al. (2019) and Armenian sector of the Arabia-Eurasia by Sugden et al. (2020) are also reported.

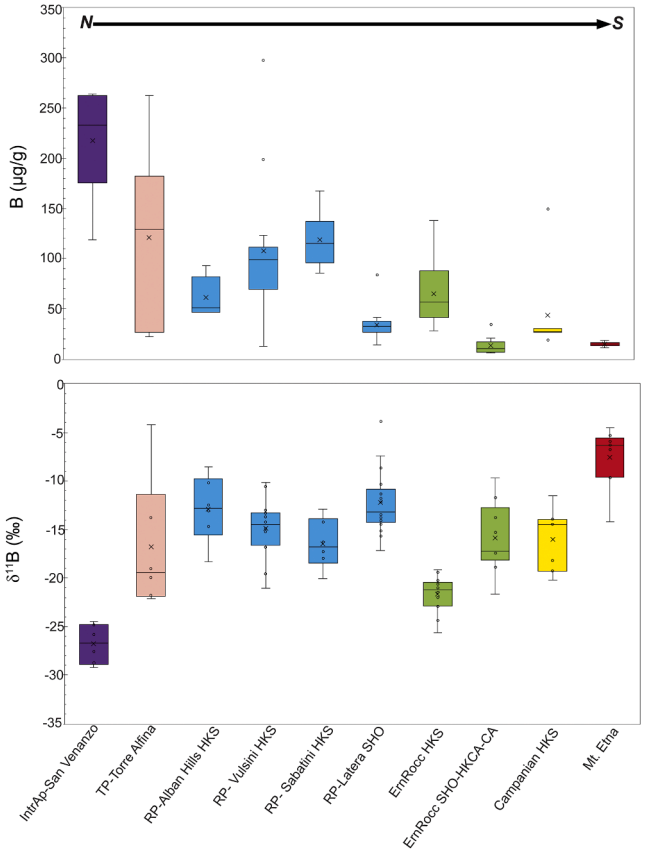

Fig. 5. [B] and δ^{11}B in the studied MIs in a standard box-and-whisker formulation. The data show a decrease of [B] and a relative increase of δ^{11}B values from the northern to the southern Italian magmatic provinces. IntrAp: Intra-Apennine province; TP: Tuscan province; RP: Roman province; ErnRocc: Ernici-Roccamonfina province. HKS: high-K series; SHO: shoshonitic series; HKCA: high-potassium calc-alkaline series; CA: calc-alkaline.

MIs vs. 6–34 µg/g for Ernici-Roccamonfina SHO MIs). The MIs from Mt. Etna overlap with the whole rock data reported by Tonarini et al. (2001) and the olivine-hosted melt inclusions from Stromboli volcano in the southern Italian Aeolian Islands, as reported by Schiavi et al. (2012).

5. Discussion

5.1. Boron in a post-collisional setting

The B isotope data presented above have a unique range of compositions. The strongly negative δ^{11}B values and the wide range of [B] in MIs trapped in high-Fo olivine from Italian magmatism (−29.2 to −3.9‰ and from 4 to 298 µg/g, respectively) are highly variable and they are incompatible with derivation from a MORB (Marschall et al., 2017) or OIB source (Walowski et al., 2021) and are isotopically lighter than worldwide volcanic arcs (Fig. 4). The B isotope data are also inconsistent with contamination by seawater (+39.6‰; Foster et al., 2010; Fig. 4).

Boron, is an effective tracer of crustal recycling processes and pathways. Although B concentrations and isotope signatures of arcs are well studied, B data from post-collisional settings are scarce. The Italian magmatism likely records mantle modified by subducted crustal material transferred into the overlying mantle wedge resulting in strong trace element enrichment and continental crust-like isotopic signatures (e.g., Conticelli et al., 2002, 2015; Avanzinelli et al., 2009; Peccerillo, 2005, 2017; Günther et al., 2023). Part of our data are comparable with B concentrations in potassic and ultrapotassic rocks from the Anatolia continental-collision setting (Palmer et al., 2019). δ^{11}B values reported on whole rocks by Palmer et al. (2019) range from −31.3 to +6.1‰, and [B] from 3.4 to 74.8 µg/g. Also, data on δ^{11}B and [B] µg/g (coupled with δ^{7}Li analysis) for ultrapotassic rocks in western Anatolia by Agostini et al. (2008) show similar negative B isotope ratio (δ^{11}B −15 to −11‰; [B]=24–30 µg/g). In contrast, results from analyses of rock samples by Sugden et al. (2020) from the Armenian sector of the Arabia-Eurasia active collision show heavier δ^{11}B values (−5 to +2‰) than MORB. Gou et al. (2017) report B isotope data ranging from −12.5 to −10.5‰ for δ^{11}B on tourmaline from the northern and southern Tibet post-collisional setting. Thus, none of the previous studies on post-collisional magmas reported strongly negative B values combined with [B] higher than 75 µg/g, making the Roman magmatic province, Tuscan province (Torre Alfina), Ernici-Roccamonfina and San Venanzo

with $\delta^{11}B$ down to −29.2‰ and [B] up to 300 μg/g, exceptional. In the next section the regional variability is evaluated based on relations between B isotopes and concentrations, trace elements and volatiles to understand the processes involved in sediment transfer and magma genesis.

5.2. Geographical variability of B

$\delta^{11}B$ values of MIs from the various Italian magmatic provinces show a systematic north-south geographical trend (Fig. 5). The northernmost San Venanzo volcanic centre has relatively low $\delta^{11}B$, whereas Mt. Etna in the south has relatively high $\delta^{11}B$. B concentrations record a similar regional trend: B-rich MIs in the north and lower [B] in the southern-provinces MIs.

Superimposed on the broad geographical trend are local relations between K_2O, and [B], as expressed by differences between HKS and SHO-MIs (Fig. 6). Relatively low K_2O magmas, like the SHO series from the Roman province, the SHO—HKCA series from Ernici-Roccamonfina and the CA series from Mt. Etna, are characterized by the lower [B] (with higher contents in the northern part of the Roman province SHO). In contrast, high-potassic ($K_2O > 4$ wt.%) magmas show a wide range in B contents, high [B] (50–140 μg/g) in Ernici-Roccamonfina HKS, and Roman province HKS melts characterized by [B] between 50 and 300 μg/g, with B increasing from the low potassic HKS member to the highest potassic kamafugites. Campania HKS melts have the lowest [B] (< 40 μg/g).

Fig. 7 presents the variation of $\delta^{11}B$ and [B] with Cl (wt.%) content for the studied MIs. The B/Cl is commonly used to evaluate the effects of melting and mineral fractionation as Cl is an incompatible element in mantle minerals. Our observations reveal that the northern provinces (San Venanzo, Torre Alfina, and the HKS from the Roman province and Ernici Roccamonfina) exhibit the lowest Cl (wt.%) content.

Within the Ernici-Roccamonfina province, the HKS and SHO compositions display distinct trends. The SHO MIs have higher Cl (wt.%) with [B] values <34 μg/g, whereas the HKS compositions exhibit higher [B] (up to 102 μg/g) with corresponding lower Cl (wt.%). Furthermore, the $\delta^{11}B$ values for the HKS in Ernici-Roccamonfina are more negative compared to the SHO compositions.

In contrast, the Campanian province, despite having similarly negative $\delta^{11}B$ values as the other peninsular magmatic provinces, exhibits the highest Cl (wt.%) values. This observation suggests that, based on $\delta^{11}B$, these provinces may share a common source, while the high Cl content in the Campanian province signifies the influence of an additional contributing factor. Cl is utilized as a tracer for fluid involvement (e.g., John et al., 2010; Keppler, 2017) due to its preferential incorporation into the fluid phase. Therefore, high Cl (wt.%) content is associated with the enrichment of subduction-derived fluids in the magma source (Fabbrizio et al., 2013). Our data are in line with the conclusions

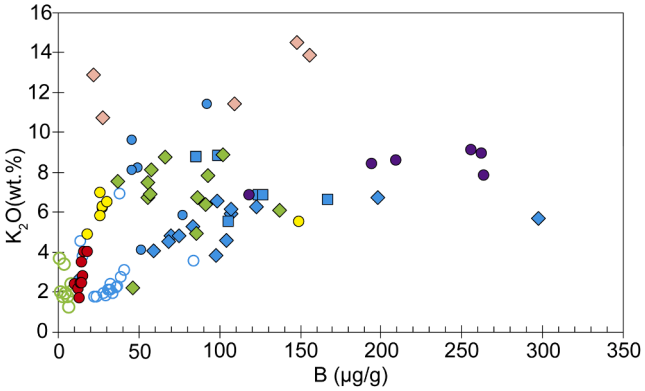

Fig. 6. Variation of K_2O (wt.%) vs. B (μg/g) in the studied MIs. Symbols as in Fig. 2.

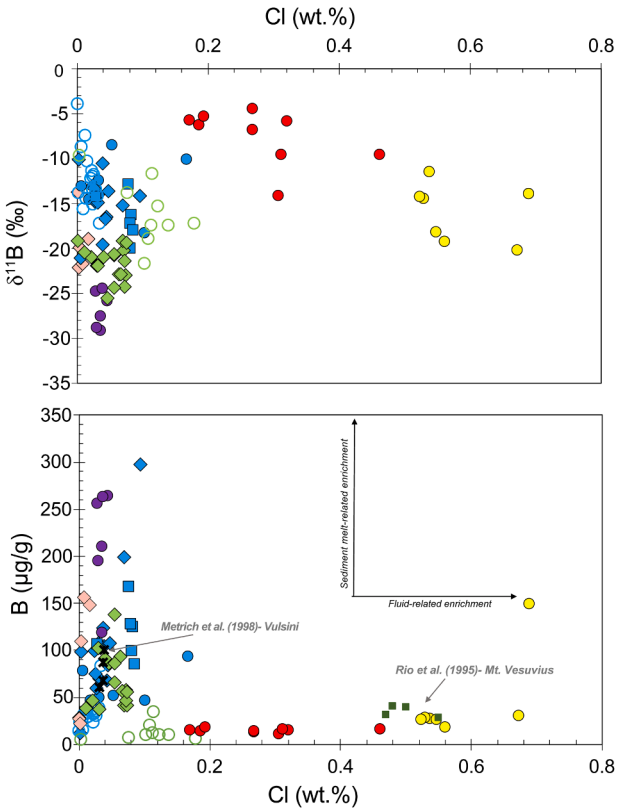

Fig. 7. (a-b). Boron isotope composition and content vs. Cl (wt.%) in the studied MIs. Data on MIs from Vulsini (Roman province; Metrich et al., 1998) and on glass inclusions Mt. Vesuvius (Rio et al., 1995). Symbols that are not in the legend as in Fig. 2.

of Metrich et al. (1998) and Rio et al. (1995; Fig. 7b), supporting that the source of the Campanian province has high Cl content due to greater fluid input.

Based on boron content, $\delta^{11}B$ and major element data (Fig 7) we can make the following geographical distinction: i) The northern-central provinces including the San Venanzo, Torre Alfina, and part of Roman Province and Ernici-Roccamonfina HKS data have low Cl (wt.%), relatively negative $\delta^{11}B$ values (Fig.7a) and higher B content; ii) Mt. Etna MIs has low Cl (wt.%) and the lowest [B] (μg/g) and $\delta^{11}B$ values; and iii) the Campanian province has $\delta^{11}B$ comparable with the Roman province and Ernici-Roccamonfina SHO but [B] slightly above the Mt. Etna MIs and the highest Cl (wt.%).

Trace element systematics support the hypothesis of the variable role of volatiles in magma production. Elements such as large-ion lithophile elements (LILE; Rb, Sr, Ba and Cs) are transported with fluids derived by dehydration of the subducted lithosphere, while Th, as well as the light REEs (LREEs), mainly migrate in melts (e.g., Johnson and Plank, 2000). Th is therefore a proxy of recycled sediment, and high Th/Nb provides evidence for the contribution of recycled sediments to the melts (e.g., Johnson and Plank, 2000). In contrast, elevated Ba/Th is considered an indicator of a fluid-dominated subduction component in the melt source (e.g., Hawkesworth et al., 1997; Elliott et al., 1997; Avanzinelli et al., 2008; Fig. 8a). In Fig. 8a and 8b we report Th/Nb vs. Ba/Th and Ce/B vs. Ba/Th in the studied MIs. B and Ce have similar incompatibilities, and the relations between Ce/B and $\delta^{11}B$ serve as a reliable method for evaluating the involvement of subducted materials during mantle melting (e.g., de Hoog and Savov, 2018).

MIs with low Cl (wt.%) but high [B] (μg/g) from the Roman province, Ernici-Roccamonfna HKS and San Venanzo have elevated Th/Nb and lower Ba/Th. These characteristics, widely reported in the literature for subduction-related ultrapotassic rocks, are indicative of recycled

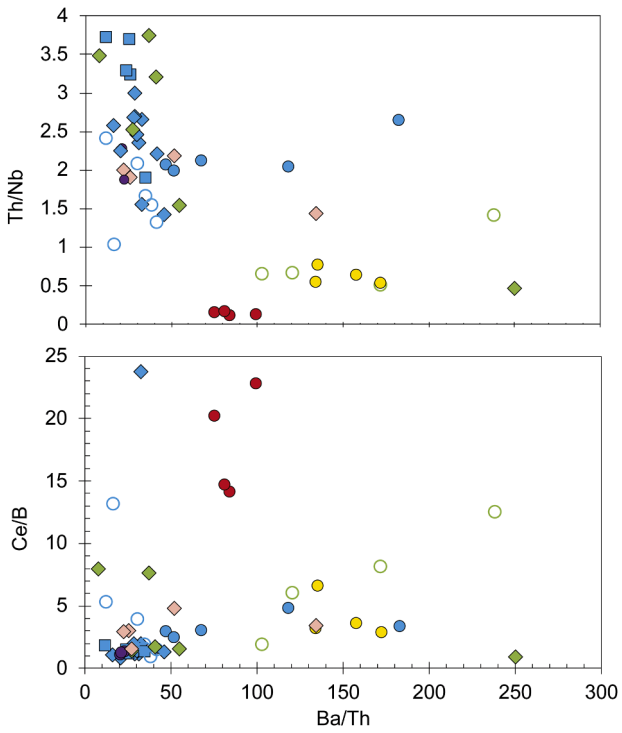

Fig. 8. (a-b). Th/Nb vs. Ba/Th and Ce/B vs. Ba/Th in the studied MIs. In Fig. 8a, Th/Nb vs. Ba/Th represent proxies of recycled sediment and fluid enrichment, respectively, whereas B and Ce have similar incompatibilities, and Ce/B is sensitive to slab contributions. Symbols as in Fig. 2.

sediment within their mantle source transferred as melts rather than aqueous fluids (e.g., Plank and Langmuir, 1993; Elliott et al., 1997; Avanzinelli et al., 2008, 2009) and are in agreement with our data from the northern provinces. In contrast, MIs with high Cl (wt.%) and low [B] (μg/g) from Campanian and Ernici-Roccamonfina SHO have lower Th/Nb and higher Ba/Th confirming the input of a fluid-dominated melt source (Fig. 8a). Mt. Etna samples have the lowest Th/Nb, possibly due to a negligible contribution of sediments in the source. In contrast, Mt. Etna MIs show higher Ba/Th content than the northern provinces indicating a fluid component, but values are slightly lower than the Campanian and Ernici-Roccamonfina SHO. In comparison to the other studied samples, Mt. Etna MIs exhibit a notably higher Ce/B ratio. This difference can be attributed to low [B] content and elevated [Ce], ranging between 205.6 and 371 μg/g. Conversely, the Ce/B ratios of the Roman HKS data, San Venanzo data, and a subset of the Ernici-Roccamonfina data have lower ratios between 0.9 and 4.8. The Ce/B ratios for the Tuscan, Ernici-Roccamonfina HKS, Campanian province, and additional Ernici-Roccamonfina HKS samples display higher values, ranging from 1.2 to 7.9. The SHO samples exhibit a broader range of Ce/B ratios, spanning from 0.9 to 13.2. A particular outlier from the Vulsini HKS displays an exceptionally high Ce/B ratio of 23.8 (Fig. 8b) and this is attributed to its low [B] of 12 μg/g when compared to the data obtained from the same volcano.

Based on the combined data of major and trace elements in Italian primary melts, we have interpreted the compositional variation between and within the magmatic provinces as a result of melts originating from a heterogeneous vein system in the mantle wedge, where the primitive HKS and CA–HKCA–magmas originate from distinct domains, rather than rather than arising from a common source through progressive changes in the proportion of veins during the melting process as reported in Avanzinelli et al. (2009). While we recognize that the hypothesis presented in Avanzinelli et al. (2009) can explain some of the observed intra-group variations, these factors alone cannot account for the variations observed between the different suites.

Furthermore, the observed geographical relationships within primary MI compositions reflects different inputs to the mantle sources from north to south likely as a result of variable metasomatic processes above the subducted slabs. Based on the relations between the boron data, volatile contents and trace element ratios, we distinguish three mantle end members that contributed to the diversity of the Italian magmatism 1) depleted mantle with relatively heavy $\delta^{11}B$ combined with low B (−7.1‰; [B]=0.077 μg/g; Marschall et al., 2017) and low volatile contents; 2) a fluid-enriched component with relatively heavy $\delta^{11}B$ values and high volatile content and; 3) a sediment-enriched component with high [B], strongly negative $\delta^{11}B$ and low volatile contents (Figs. 7-8).

This section explores the significance of the end members in the context of the potassic Italian magmatism. In the north, San Venanzo with low Ba, relatively high Th (see Fig. 8) and low Cl (wt.%) and Ce/B (Figs.7-8b) combined with the highest boron content and the highly negative $\delta^{11}B$ requires addition of ^{10}B-rich sediments to the source of these MIs. Based on high K_2O, trace elements, and high boron content combined with a negative B isotope ratio, we infer a sediment-related input for the source of the Torre Alfina lamproites. The sediment input must, however, differ from the source of the San Venanzo kamafugites, as the Torre Alfina MIs show relatively lower Th and U MIs (see Table S1). For Torre Alfina samples, we suggest a K-rich source modified by input of metapelites rich in ^{10}B, possibly introduced by Alpine subduction as also suggested by Conticelli and Peccerillo (1990). Previous publications (e.g., Peccerillo, 2017) suggest a harzburgite source for San Venanzo modified by addition of marly sediments from the Adriatic plate.

The Roman province $\delta^{11}B$ values and boron content record a large range and represent intermediate compositions between San Venanzo in the north and Mt. Etna in the south. Low Ba/Th and high Th/Nb suggest recycling and melting of sediments. Carbonate-rich sediments have long been proposed as a contributing factor to the overall composition of the Roman province magmas and the Neapolitan districts (Conticelli et al., 2002). Avanzinelli et al. (2008) suggested that there is an increasing proportion of carbonate in the southern regions, corresponding to the sediment composition along the Apennine chain. The incorporation of recycled carbonate-bearing pelitic sediments within the mantle wedge is supported by the absence of a negative Sr anomaly in Roman mafic rocks compared to Tuscan rocks, and it is responsible for the formation of metasomatic phlogopite-bearing wehrlitic veins in the mantle wedge. However, based on the $\delta^{11}B$ and [B] data presented in this study, it is not possible to establish a conclusive relationship between boron and subducted carbonates. Marine carbonate show $\delta^{11}B$ values between −5 and +26.2‰ (Marschall et al., 2017, and reference therein), and biogenic carbonates between +4.9 and +38.5‰ (Marschall et al., 2017, and reference therein), which excludes them as a primary factor contributing to the observed elemental and isotopic variability. Nonetheless, it is important to note that we do not exclude the presence of carbonates, rather another component (pelitic) must be responsible for their role as the main factor creating the light $\delta^{11}B$ and high [B] for the Italian MIs.

Furthermore, the low Cl (wt.%) excludes the involvement of a large fluid component in the sources of these central magmatic provinces.

The Ernici-Roccamonfina province represents a transition between the Roman and Campanian provinces. The geochemical compositions indicate that the Roman magmas represent mixing of primary melts derived from sources that show an addition of sediment whereas Campanian compositions require a minor fluid component on their source. The Ernici-Roccamonfina volcanism was likely triggered by asthenosphere mantle inflow through a slab-tear window below the Ernici-Roccamonfina province. (e.g., Faccenna et al., 2014; Koornneef et al., 2019).

Campanian province MIs indicate a fluid input to the source with a geochemical signature distinct from the mantle sources in the north. This conclusion is supported by the high Cl (wt.%) compared to the more northern provinces as well as an intermediate Ba/Th and a lower U

content. The fluid input can possibly be associated with the Ionian slab rather than the Adriatic plate (Peccerillo and Panza, 1999; Cortini et al., 2004; Peccerillo, 2017). Avanzinelli et al. (2008) based on U/Th disequilibria study on Vesuvius HKS samples suggest the involvement melts from deeply subducted carbonate-rich sediments of the Ionian slab to generate a high-U, low-Th component. Nonetheless, while Cl (wt.%) analysis suggests the input of fluids, the boron isotopic values do not exhibit any significant differences compared to the other more northern provinces, although we do observe lower boron content. We conclude that the source of the Campanian province is affected by the input of fluids, but the B isotopes values suggest that recycling of sediments similar to those of the Roman province dominates the signature of fluids in terms of B (see Section 5.3 for more details).

Mt. Etna MIs have less negative $\delta^{11}B$ and lower B contents compared to peninsular Italy MIs with compositions between MORB and the Aeolian islands (Figs. 4-5). Based on fluid-mobile elements, volatiles and boron data, the nearby Ionian subducting slab is the favoured origin of the subduction-related fluids in the Mt. Etna source. For this reason, we conclude that Mt. Etna magmatism represents an end member of the components contributing to Italian magmatism in the region. Mt. Etna activity is commonly explained by the presence of a discontinuity resulting from slab roll-back of the oceanic Ionian slab and Sicilian continental crust that generated a slab window leading to the ascent of asthenosphere beneath Mt. Etna (e.g., Doglioni et al., 2001).

The observed compositional diversity of the Italian MIs is likely caused by different source mineral assemblages and different degrees of partial melting. The heterogeneous metasomatized mantle system was influenced by a changing geodynamic setting that resulted in different sediment involvement: the north of the peninsula was mainly influenced by Alpine subduction of pelites and marls with a continental crust composition, and the centre by recycled carbonate-rich sediments from the Miocene-to-present Adriatic plate subduction (Ammannati et al., 2016; Avanzinelli et al., 2008, 2009, 2018; Conticelli et al., 2015).

In contrast, in the south there is an additional involvement of fluids and associated sediments due to active subduction of oceanic lithosphere (Ionian plate) under the Calabrian arc.

Previous studies, show how the diverse Italian magmatism results from different crustal components interacting with the mantle above the subduction zone, generating different radiogenic isotope variations (e.g., Conticelli et al., 2002; Nikogosian and van Bergen, 2010; Nikogosian et al., 2016; Koornneef et al., 2019). Compositional variations have been related to a compositionally zoned mantle with a network of veins with different mineralogies and metasomatic imprints (e.g., Frezzotti et al., 2007). In the following section we aim to explore this further based on B isotope systematics.

5.3. Sources for boron

As demonstrated in the previous two sections, the geochemical data unambiguously demonstrate the addition of subducted sediments and variable amount of fluids in the source of Italian Peninsula magmatism. The extremely negative $\delta^{11}B$ signatures are, however, unusual and require a more detailed explanation. In subduction zones, high-P mica phases such as phengite represent an important carrier of fluid-mobile trace elements including B, Li and LILE, where it is formed by metamorphic replacement of both igneous and sedimentary minerals. During progressive slab dehydration as the slab is subducted in the mantle, the heavy B isotope preferentially fractionates into aqueous fluids and leave an isotopically lighter residual phengite (e.g., Ishikawa and Nakamura 1994; Marschall et al., 2006, 2007; De Hoog and Savov, 2018). Examples of $\delta^{11}B$ values down to −29‰ and [B] between 50 and 250 μg/g are recorded in phengite from high-pressure rocks from the Luliang Shan terrane (Menold et al., 2016), whereas Marschall et al. (2006) found [B] between 43 and 136 μg/g in phengite from high-pressure metamorphic rocks from the island of Syros (Greece). Marschall et al. (2007) modelled the release of B from progressive dehydration of AOC during subduction and conclude that the B content is strongly dependant on the presence of white mica in the rock. Moreover, progressive dehydration of phengite-bearing rocks and phengite-free HP rocks under pressure between ~ 1.5 GPa and 2.5 GPa result in different $\delta^{11}B$ values. The phengite-free dehydration model results in $\delta^{11}B$ down to −30‰, whereas the phengite-bearing rock model decreases only to −8.6‰, based on the AOC composition of $\delta^{11}B$=+0.8‰ and [B]=26 μg/g (from Smith et al., 1995). However, if we consider phengite-bearing sediments with a negative isotopic ratio, e.g., ~ −13‰ (Tonarini et al., 2011), the $\delta^{11}B$ of the dehydrated sediments would shift to more negative values, e.g., ~ −21‰ for a phengite-bearing composition

MIs across the entire Italian peninsula exhibit boron isotope data with large variability towards extremely negative values, indicating a common source for all the Italian potassic series, regardless of spatial and temporal factors. Schmidt et al. (1996) demonstrated experimentally that phengite in metasediment-bearing subducting oceanic crust can carry K and B to great depths, however, when subducted slabs reach 100–300 km, phengite breaks down between 1075 and 1150 °C at 7–8 GPa and at 1000–1050 °C at 10 GPa (Thomsen and Schmidt, 2008). In the context of a post-collisional setting, slab tearing and break off will induce phengite breakdown due to heat input of asthenosphere inflow from behind the subducting slab. Consequently, we ascribe the extreme boron isotope signature in the Italian MIs can be explained by consumption of phengite from subducted sediments with strongly negative $\delta^{11}B$.

The next section integrates the observed geochemical variability across the Italian post-collisional arc within the two-stage melting model that explains the role of phengite within recycled sediment package in a more quantitative way.

5.4. Two-stage melting model

To understand how dehydration of the subducting slab and melting of sediments and the mantle wedge produced the different Italian magmas we first develop a physical mixing model that evaluates $\delta^{11}B$ with elements of similar incompatibility (Ce and B; Marschall et al., 2017; Fig. 9).

The model involves mixing between: depleted MORB mantle (DMM) representing the unmetasomatised mantle wedge ($\delta^{11}B$= −7.1‰ and

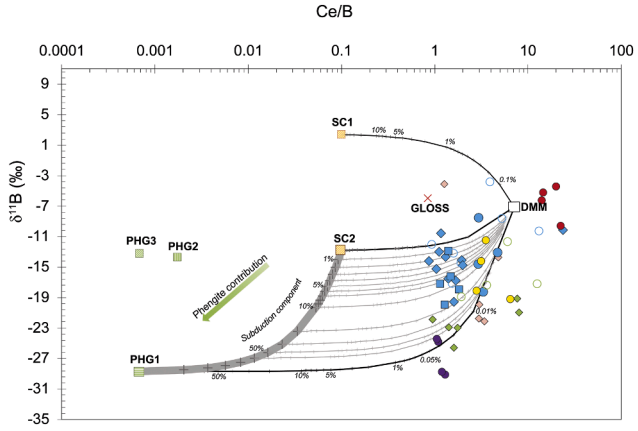

Fig. 9. $\delta^{11}B$ vs. Ce/B for the studied MIs. Calculated mixing model between DMM= depleted MORB mantle (*Marschall et al., 2017*) and subduction components containing various amount of phengite. Subduction Component 1 (SC1) and Subduction Component 2 (SC2), respectively $\delta^{11}B$=+2.4‰ and $\delta^{11}B$= −12.8‰ after *Tonarini et al. (2011)*; Ce/*B* = 0.1 after *Iveson et al. (2021)*. Phengite 1 with $\delta^{11}B$= −28.7‰ and Ce/*B* = 0.0006 (*Menold et al., 2016*; *Xu et al., 2022*). For comparison composition of phengite reported by *Klemme et al. (2011*; PHG2; $\delta^{11}B$= −13.7‰; Ce/*B* = 0.0006) and from *Xu et al. (2022*; PHG3; $\delta^{11}B$= −13.3‰, Ce/*B* = 0.14) have been shown. GLOSS (red cross; *Plank, 2014*).

Ce/B = 7.14; Marschall et al., 2017) and a subduction component, that includes the residual slab after progressive subduction zone dehydration up to 120 km depth with low [B] and δ^{11}B (SC2; [B]=16.8 μg/g, δ^{11}B= −12.8‰; Tonarini et al., 2011) and different proportion of phengite (PHG1) from high pressure subduction environment after Menold et al. (2016; δ^{11}B= −28.7‰; Ce/B = 0.0006).

Mixing line between DMM and pre-hydration subduction component (SC1) represented by the starting composition for an uppermost slab (composed by 90% AOC and 10% sediment; after Tonarini et al., 2011; [B]=35 μg/g, δ^{11}B=+2.4‰) show that no fluids are involved in the source of the Italian MIs. The Ce/B of SC1 and SC2 (Ce/B = 0.1) are from Iveson et al. (2021). For comparison, we report different phengite compositions from the literature: Phg2: δ^{11}B= −13.7‰; Ce/B = 0.0017 (Klemme et al., 2011); Phg3: δ^{11}B= −13.3‰; Ce/B = 0.0006; (Xu et al., 2022).

Fig. 9 shows the outcome of mixing the phengite composition from Menold et al. (2016) that has the most negative δ^{11}B with DMM and with the two subduction components to reflect the presence of phengite within the metamorphosed sediments. To explain the most extreme δ^{11}B MI data in Fig. 9 small amounts of light phengite (< 0.04%) are required in the subduction component, e.g., San Venanzo requires ~0.03% phengite. The other Italian post-collisional melts generally plot above the mixing line between DMM and the most extreme phengite composition and imply greater involvement of SC2 although almost no data imply a role for fluids derived from non-dehydrated oceanic crust, with the exception of one outlier from Torre Alfina plotting in the range between SC1 and DMM mixing. Roman and Ernici-Roccamonfina province HKS melts reflect a mixture between mantle wedge DMM and contribution between 0.01–0.03% of phengite within the subduction component. In contrast, Torre Alfina, Campanian province data and Ernici-Roccamonfina province SHO require a smaller contribution of phengite (<0.01%). Data from Roman province SHO suggest the involvement up to 0.03%.

We suggest that the provinces with the larger involvement of the hypothetical phengite-bearing subduction component in the north of the peninsula are influenced by the subduction of clay-rich- sediments that were metamorphosed to phengite during the Alpine and Adria subduction. The Mt. Etna melts, in the south have higher Ce/B than DMM but comparable δ^{11}B from DMM values, suggesting a minimal or no role for a phengite- bearing subduction component. Instead, a different process is required to enrich the Ce/B for Mt. Etna.

The mixing model implies that phengite plays a major role in producing the highly negative δ^{11}B for the analysed Italian MIs whereas the role of dehydrated fluids seems negligible, in line with Cl (wt.%) data presented in Fig. 7. To explain the strong phengite signature in the MIs data inferred from the bulk mixing model requires a two-stage melting model that initially transfers the phengite from the subducted slab to the mantle wedge which subsequently undergoes melting to produce the magmatism in the Italian post-collisional setting. We propose:

1) Slab break-off induced sediment melting to depths >100 km after an early stage of oceanic crust consumption and dehydration that included at least part of its sediment cover. The phengite hosted in the subducted sediments was depleted in ^{11}B due to dehydration, producing strongly negative δ^{11}B signatures. The inflow of hot asthenosphere following slab break-off, initiated phengite breakdown responsible for the release of the negative boron isotope signature. The generated melts are strongly enriched in K and in other mobile elements such as B, Rb, U, Pb. The transfer of these melts into the overlying mantle results in reaction with the depleted mantle wedge to cause the formation of metasomatic veins containing K-rich phases like phlogopite (e.g., Foley, 1992; Melzer and Foley, 2000; Mazzeo et al., 2014). The sediments containing the phengite vary in composition and abundance from north (metapelite and marls) to south (marls, Section 5.2; Fig. 10). Our model requires that the negative boron and high boron concentration are transferred from melts of phengite bearing sediments at depth into the K-rich phases in the overlying mantle wedge.

1) Partial melting of the veined lithosphere occurred due to further opening of the slab window and the increase of the heat from the inflowing asthenosphere with the tear widening from north to south (e.g., Nikogosian and van Bergen, 2010; Spakman and Wortel, 2004). This second stage is required to explain the extreme geochemical variability observed in the olivine-hosted MIs (extreme K_2O enrichments and variable Th/Nb) that require the melt source to be mineralogically heterogeneous on a small scale. Partial melting of this veined source rich in hydrous phases such as phlogopite and amphibole (e.g., Foley, 1992, 1999) results in the strong enrichments in highly incompatible elements.

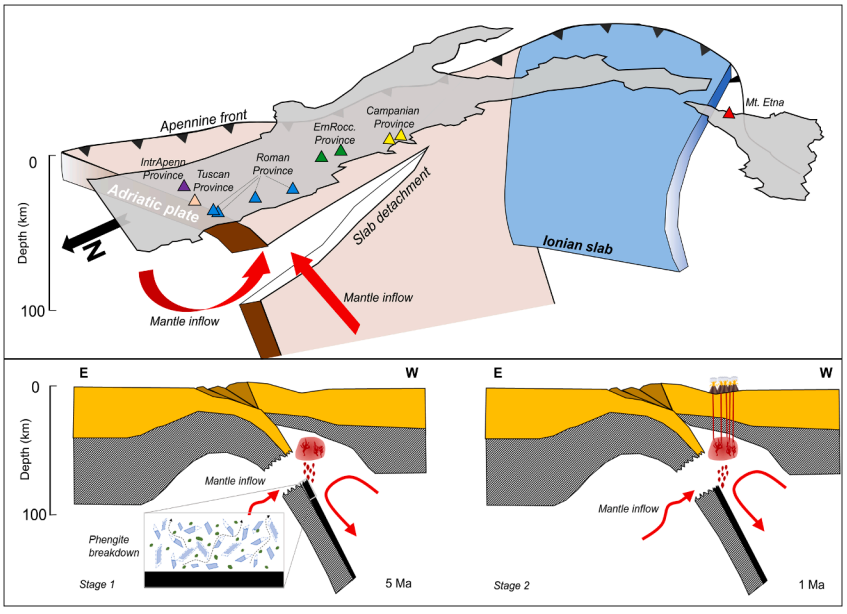

Fig. 10. a) Schematic view summarising the main features and processes in the mantle wedge beneath Italy responsible for the characteristic magmatism. b) Cartoon illustrating the two-stage melting process of Italian magmatism based on boron data in high- forsterite MIs: stage 1) the slab detachment and subsequent mantle inflow increase the temperature and induce phengite breakdown (zoomed square) from the AOC portion (black layer); stage 2) Melting of overlying veined lithosphere due to the slab window.

The more negative $\delta^{11}B$ in the north suggests a greater phengite contribution, possibly due to higher temperature induced by a larger input of asthenosphere inflow in northern Italy where the tear is wider (Rosenbaum et al., 2008) and/or by the more pelitic sediment composition. The southern magmatic provinces with a less negative boron isotope signature, as well as lower boron content, which suggest a less pronounced role for phengite breakdown or less phengite. Mt. Etna is characterised by a boron signature similar to a MORB-like source suggesting no phengite contribution (Fig. 10).

In conclusion, the two-stage model presented in this study provides a mechanism to explain the extreme enrichment of K (and Th) in combination with the negative $\delta^{11}B$ observed in melt inclusions. Transfer of sediments through a relatively cool mélange diapir (Behn et al., 2011; Marschall and Schumacher 2012; Peccerillo and Frezzotti, 2015) is less likely to explain the extreme observed enrichments and heterogeneity, as a cool rising diapir would not instigate phengite breakdown to provide the boron signatures. In the diapir model the transportation of sediments is proposed to occur within mélanges consisting of subducted rocks and peridotites. Ascent of these relatively cool mélange diapirs is envisioned through Rayleigh-Taylor instability, which then undergo dehydration and melting in the hotter mantle wedge to react with the surrounding mantle. The slab tear under Italy, however, provides a heat source that directly causes phengite breakdown and melting of the sediment pile at depth after they have undergone extensive dehydration, to be transferred to wedge where it reacts and crystallises in a vein network. Those veins subsequently melt partially due to a rise in T associated with further opening of the slab window. This second stage partial melting process is crucial for achieving the observed extreme enrichment in K and Th.

Conclusions

Boron content and isotope composition of melt inclusions in high-forsterite olivine from Italian magmatic provinces constrain the nature of the mantle source of these melts and the processes involved in their production and transfer from mantle to crust. The high boron content and the negative $\delta^{11}B$ are unique and distinct compared to magmatism from arcs or other post-collisional settings magmatism. Major, trace and volatile elements indicate input of sediments and variable amount of fluids to the mantle source.

The strongly negative $\delta^{11}B$ values derive from a common source in all the Italian MIs (with the exception for Mt. Etna), which is interpreted as phengite, a white mica stable to high pressures in the sediments of altered oceanic crust that underwent dehydration and ^{11}B depletion. The heat generated by the asthenosphere upwelling associated with slab detachment is responsible for phengite breakdown and the release of a negative $\delta^{11}B$ signature to the overlying mantle. Our data suggest that the boron signature from this phase survives despite the transfer and the depth. K-rich melts generated from this process reacted with the overlying depleted mantle wedge and led to a variably metasomatized source. A mixing model based on Ce/B and $\delta^{11}B$ suggests the influence of various proportions of the DMM, an AOC slab and sediment component including phengite (0–0.4%) is required to explain the variable geochemistry observed in the Italian Mis. The model also indicates that Mt. Etna data saw no significant influence from the subduction component or phengite. A two-stage melting model is required to explain the extreme K and trace element contents of the MIs with initial transfer of sediment-derived melts into a vein network and subsequent partial melting of those veins is required to explain the extreme enrichments of K and trace elements.

CRediT authorship contribution statement

Natascia Luciani: Writing – original draft, Visualization, Formal analysis, Data curation. **Igor K. Nikogosian:** Resources, Investigation, Data curation. **Cees-Jan De Hoog:** Investigation, Writing – review & editing. **Gareth R. Davies:** Writing – review & editing. **Janne M. Koornneef:** Funding acquisition, Writing – review & editing, Conceptualization.

Declaration of Competing Interest

The authors declare that they have no known competing financial interests or personal relationships that could have appeared to influence the work reported in this paper.

Data availability

The data are shared at the Attachment file step

Acknowledgments

The authors thank Helen de Waard and Eric Hellebrand for LA-ICP-MS and EMPA analyses, respectively. N.L. thank Roel van Elsas and Antoine J. J. Bracco Gartner for their help with the mineral separation. We would like to thank the editor Rosemary Hickey-Vargas and the reviewer H. Marschall and the second reviewer for their helpful and constructive comments and suggestions. The research leading to these results has received funding from the European Research Council (ERC) under the European Union's Horizon 2020 research and innovation program (grant agreement 759563)

Supplementary materials

Supplementary material associated with this article can be found, in the online version, at doi:10.1016/j.epsl.2023.118462.

References

Ammannati, E., Jacob, D.E., Avanzinelli, R., Foley, S.F., Conticelli, S., 2016. Low Ni olivine in silica-undersaturated ultrapotassic igneous rocks as evidence for carbonate metasomatism in the mantle. Earth Planet. Sci. Lett. 444, 64–74.

Agostini, S., Ryan, J.G., Tonarini, S., Innocenti, F., 2008. Drying and dying of a subducted slab: coupled Li and B isotope variations in Western Anatolia Cenozoic Volcanism. Earth Planet. Sci. Lett. 272 (1–2), 139–147.

Avanzinelli, R., Elliott, T., Tommasini, S., Conticelli, S., 2008. Constraints on the genesis of potassium-rich Italian volcanic rocks from U/Th disequilibrium. J. Petrol. 49 (2), 195–223.

Avanzinelli, R., Lustrino, M., Mattei, M., Melluso, L., Conticelli, S., 2009. Potassic and ultrapotassic magmatism in the circum-Tyrrhenian region: significance of carbonated pelitic vs. pelitic sediment recycling at destructive plate margins. Lithos 113 (1–2), 213–227. https://doi.org/10.1016/j.lithos.2009.03.029.

Avanzinelli, R., Casalini, M., Elliott, T., Conticelli, S., 2018. Carbon fluxes from subducted carbonates revealed by uranium excess at Mount Vesuvius. Italy. Geology 46 (3), 259–262.

Behn, M.D., Kelemen, P.B., Hirth, G., Hacker, B.R., Massonne, H.J., 2011. Diapirs as the source of the sediment signature in arc lavas. Nat. Geosci. 4 (9), 641–646.

Berndt, M.E., Seyfried Jr, W.E., 1990. Boron, bromine, and other trace elements as clues to the fate of chlorine in mid-ocean ridge vent fluids. Geochim. Cosmochim. Acta 54 (8), 2235–2245.

Carminati, E., Doglioni, C., 2012. Alps vs. Apennines: the paradigm of a tectonically asymmetric Earth. Earth Sci. Rev. 112 (1–2), 67–96. https://doi.org/10.1016/j.earscirev.2012.02.004.

Conticelli, S., Peccerillo, A., 1990. Petrological significance of high-pressure ultramafic xenoliths from ultrapotassic rocks of Central Italy. Lithos 24 (4), 305–322.

Conticelli, S., D'antonio, M., Pinarelli, L., Civetta, L, 2002. Source contamination and mantle heterogeneity in the genesis of Italian potassic and ultrapotassic volcanic rocks: Sr–Nd–Pb isotope data from Roman Province and Southern Tuscany. Mineral. Petrol. 74 (2), 189–222.

Conticelli, S., Guarnieri, L., Farinelli, A., Mattei, M., Avanzinelli, R., Bianchini, G., Boari, E., Tommasini, S., Tiepolo, M., Prelević, D., Venturelli, G., 2009. Trace elements and Sr-Nd-Pb isotopes of K-rich, shoshonitic, and calc-alkaline magmatism of the Western Mediterranean region: genesis of ultrapotassic to calc-alkaline magmatic associations in a post-collisional geodynamic setting. Lithos 107 (1–2), 68. https://doi.org/10.1016/j.lithos.2008.07.016, 92.

Conticelli, S., Avanzinelli, R., Ammannati, E., Casalini, M., 2015. The role of carbon from recycled sediments in the origin of ultrapotassic igneous rocks in the Central Mediterranean. Lithos 232, 174–196.

Cortini, M., Ayuso, R.A., De Vivo, B., Holden, P., Somma, R., 2004. Isotopic composition of Pb and Th in interplinian volcanics from Somma–Vesuvius volcano. Italy. Mineral. Petrol. 80, 83–96.

D'Antonio, M., Civetta, L., Di Girolamo, P., 1999. Mantle source heterogeneity in the Campanian Region (South Italy) as inferred from geochemical and isotopic features of mafic volcanic rocks with shoshonitic affinity. Mineral. Petrol. 67, 163–192.
Danyushevsky, L.V., Della-Pasqua, F.N., Sokolov, S., 2000. *Re*-equilibration of melt inclusions trapped by magnesian olivine phenocrysts from subduction-related magmas: petrological implications. Contrib. Mineral. Petrol. 138 (1), 68–83.
Danyushevsky, L.V., Plechov, P., 2011. Petrolog3: integrated software for modeling crystallization processes. Geochem. Geophys. Geosyst. 12 (7).
De Hoog, J.C.M., Mason, P.R.D., van Bergen, M.M., 2001. Sulfur and chalcophile elements in subduction zones: constraints from a laser ablation ICP-MS study of melt inclusions from Galunggung Volcano, Indonesia. Geochim. Cosmochim. Acta 65 (18), 3147–3164.
De Hoog, J.C.M., Savov, I.P., 2018. Boron Isotopes as a Tracer of Subduction Zone Processes. Boron Isotopes, pp. 217–247.
Doglioni, C., Innocenti, G., and Mariotti, F. (2001). Why Mt Etna? Terra Nova, 13(1), 25–31. doi:10.1046/j.1365-3121.2001.00301.x.
Elliott, T., Plank, T., Zindler, A., White, W., Bourdon, B., 1997. Element transport from slab to volcanic front at the Mariana arc. J. Geophys. Res.: Solid Earth 102 (B7), 14991–15019.
Fabbrizio, A., Stalder, R., Hametner, K., Günther, D, 2013. Experimental chlorine partitioning between forsterite, enstatite and aqueous fluid at upper mantle conditions. Geochim. Cosmochim. Acta 121, 684–700.
Faccenna, C., Becker, T.W., Auer, L., Billi, A., Boschi, L., Brun, J.P., Capitanio, F.A., Funiciello, F., Horvàth, F., Jolivet, L., Piromallo, C., Royden, L., Rossetti, F., Serpelloni, E., 2014. Mantle dynamics in the Mediterranean. Rev. Geophys. 52 (3), 283–332.
Foley, S.F., 1992. Vein-plus-wall-rock melting mechanisms in the lithosphere and the origin of potassic alkaline magmas. Lithos 28 (3–6), 187, 20.
Foley, S., Musselwhite, D., Van der Laan, S.R., 1999. Melt compositions from ultramafic vein assemblages in the lithospheric mantle: a comparison of cratonic and non-cratonic settings. In: International Kimberlite Conference. Red Roof Design, pp. 238–246, 7th: 1998.
Ford, C.E., Russell, D.G., Craven, J.A., Fisk, M.R., 1983. Olivine-liquid equilibria: temperature, pressure and composition dependence of the crystal/liquid cation partition coefficients for Mg, Fe2+, Ca and Mn. J. Petrol. 24 (3), 256–266.
Foster, G.L., Pogge Von Strandmann, P.A.E., Rae, J.W.B, 2010. Boron and magnesium isotopic composition of seawater. Geochem. Geophys. Geosyst. 11 (8), 1–10. https://doi.org/10.1029/2010GC003201.
Frezzotti, M.L., De Astis, G., Dallai, L., Ghezzo, C., 2007. Coexisting calc-alkaline and ultrapotassic magmatism at Monti Ernici, Mid Latina Valley (Latium, central Italy). Eur. J. Mineral. 19 (4), 479–497.
Gou, G.N., Wang, Q., Wyman, D.A., Xia, X.P., Wei, G.J., Guo, H.F., 2017. In situ boron isotopic analyses of tourmalines from Neogene magmatic rocks in the northern and southern margins of Tibet: evidence for melting of continental crust and sediment recycling. Solid Earth Sci. 2 (2), 43–54.
Guo, S., Su, B., John, T., Zhao, K., Tang, P., Chen, Y., Li, Y., 2022. Boron release and transfer induced by phengite breakdown in subducted impure metacarbonates. Lithos 408, 106548.
Günther, J., Prelević, D., Mertz, D.F., Rocholl, A., Mertz-Kraus, R., Conticelli, S., 2023. Subduction-legacy and olivine monitoring for mantle-heterogeneities of the sources of ultrapotassic magmas: the Italian case study. Geochem. Geophys. Geosyst. 24 (3), e2022GC010709.
Halama, R., Konrad-Schmolke, M., Sudo, M., Marschall, H.R., Wiedenbeck, M., 2014. Effects of fluid–rock interaction on $^{40}Ar/^{39}Ar$ geochronology in high-pressure rocks (Sesia-Lanzo Zone, Western Alps). Geochim. Cosmochim. Acta 126, 475–494.
Harder, H., 1970. Boron content of sediments as a tool in facies analysis. Sediment. Geol. 4 (1–2), 153–175.
Hawkesworth, C.J., Turner, S.P., McDermott, F., Peate, D.W., Van Calsteren, P., 1997. U-Th isotopes in arc magmas: implications for element transfer from the subducted crust. Science 276 (5312), 551–555.
Ishikawa, T., Nakamura, E., 1993. Boron isotope systematics of marine sediments. Earth Planet. Sci. Lett. 117 (3–4), 567–580. https://doi.org/10.1016/0012-821X(93)90103-G.
Ishikawa, T., Nakamura, E., 1994. Origin of the slab component in arc lavas from across-arc variation of B and Pb isotopes. Nature 370 (6486), 205–208.
Ishikawa, T., Tera, F, 1999. Two isotopically distinct fluid components involved in the Mariana arc: evidence from Nb/B ratios and B, Sr, Nd, and Pb isotope systematics. Geology 27 (1), 83–86.
Iveson, A.A., Humphreys, M.C., Savov, I.P., De Hoog, J.C., Turner, S.J., Churikova, T.G., Macpherson, C.G., Mather, T.A., Gordeychik, B.N., Tomanikova, L., Agostini, S., Hammond, K., Pyle, D.M., Cooper, G.F., 2021. Deciphering variable mantle sources and hydrous inputs to arc magmas in Kamchatka. Earth Planet. Sci. Lett. 562, 116848.
Kamenetsky, V.S., Sobolev, A.V., Eggins, S.M., Crawford, A.J., Arculus, R.J., 2002. Olivine-enriched melt inclusions in chromites from low-Ca boninites, Cape Vogel, Papua New Guinea: evidence for ultramafic primary magma, refractory mantle source and enriched components. Chem. Geol. https://doi.org/10.1016/S0009-2541(01)00380-1.
Kent, A.J.R., 2008. Melt inclusions in basaltic and related volcanic rocks. Rev. Mineral. Geochem. https://doi.org/10.2138/rmg.2008.69.8.
Keppler, H., 2017. Fluids and trace element transport in subduction zones. Am. Mineral. 102 (1), 5–20.
Klemme, S., Marschall, H.R., Jacob, D.E., Prowatke, S., Ludwig, T., 2011. Trace-element partitioning and boron isotope fractionation between white mica and tourmaline. Can. Miner. 49 (1), 165–176.
Konrad-Schmolke, M., Halama, R., 2014. Combined thermodynamic-geochemical modeling in metamorphic geology: boron as tracer of fluid-rock interaction. Lithos 208–209, 393–414. https://doi.org/10.1016/j.lithos.2014.09.021.
Koornneef, J.M., Nikogosian, I., van Bergen, M.J., Smeets, R., Bouman, C., Davies, G.R., 2015. TIMS analysis of Sr and Nd isotopes in melt inclusions from Italian potassium-rich lavas using prototype $10^{13}\Omega$ amplifiers. Chem. Geol. 397, 14–23. https://doi.org/10.1016/j.chemgeo.2015.01.005.
Koornneef, J.M., Nikogosian, I., van Bergen, M.J., Vroon, P.Z., Davies, G.R., 2019. Ancient recycled lower crust in the mantle source of recent Italian magmatism. Nat. Commun. 10 (1), 1–10.
John, T., Layne, G.D., Haase, K.M., Barnes, J.D., 2010. Chlorine isotope evidence for crustal recycling into the Earth's mantle. Earth Planet. Sci. Lett. 298, 175–182. https://doi.org/10.1016/j.epsl.2010.07.039 v.
Johnson, M.C., Plank, T., 2000. Dehydration and melting experiments constrain the fate of subducted sediments. Geochem. Geophys. Geosyst. 1 (12).
Chapter 12 Leeman, W.P., Sisson, V.B., 2018. Geochemistry of boron and its implications for crustal and mantle processes. In: Anovitz, L.M., Grew, E.S. (Eds.), Boron: Mineralogy, Petrology, and Geochemistry, pp. 645–708. https://doi.org/10.1515/9781501509223-014.
Marschall, H.R., Altherr, R., Ludwig, T., Kalt, A., Gméling, K., Kasztovszky, Z., 2006. Partitioning and budget of Li, Be and B in high-pressure metamorphic rocks. Geochim. Cosmochim. Acta 70 (18), 4750–4769. https://doi.org/10.1016/j.gca.2006.07.006.
Marschall, H.R., von Strandmann, P.A.P., Seitz, H.M., Elliott, T., Niu, Y., 2007. The lithium isotopic composition of orogenic eclogites and deep subducted slabs. Earth Planet. Sci. Lett. 262 (3–4), 563–580.
Marschall, H.R., 2018. Boron isotopes in the ocean floor realm and the mantle. Boron Isotopes: Fifth Element 189–215.
Marschall, H.R., Schumacher, J.C., 2012. Arc magmas sourced from mélange diapirs in subduction zones. Nat. Geosci. 5 (12), 862–867.
Marschall, H.R., Wanless, V.D., Shimizu, N., Pogge von Strandmann, P.A.E., Elliott, T., Monteleone, B.D., 2017. The boron and lithium isotopic composition of mid-ocean ridge basalts and the mantle. Geochim. Cosmochim. Acta 207. https://doi.org/10.1016/j.gca.2017.03.028.
Mason, P.R., Nikogosian, I.K., and van Bergen, M.J. (2008). Major and trace element analysis of melt inclusions by laser ablation ICP-MS. Laser ablation ICP-MS in the earth sciences: current practices and outstanding issues: mineralogical association of Canada short course series, 40, 219–240.
Mazzeo, F.C., D'Antonio, M., Arienzo, I., Aulinas, M., Di Renzo, V., Gimeno, D, 2014. Subduction-related enrichment of the Neapolitan volcanoes (Southern Italy) mantle source: new constraints on the characteristics of the slab-derived components. Chem. Geol. https://doi.org/10.1016/j.chemgeo.2014.08.014.
Maurel, C., Maurel, P., 1982. Étude expérimentale de la distribution de l'aluminium entre bain silicaté basique et spinelle chromifère. Implications pétrogénétiques: teneur en chrome des spinelles. Bull. Miner. 105 (2), 197–202.
Melzer, S., Foley, S.F., 2000. Phase relations and fractionation sequences in potassic magma series modelled in the system $CaMgSi_2O_6$-$KAlSiO_4$-Mg_2SiO_4-SiO_2-F_2O^{-1} at 1bar to 18 kbar. Contrib. Mineral. Petrol. 138, 186–197.
Menold, C.A., Grove, M., Sievers, N.E., Manning, C.E., Yin, A., Young, E.D., Ziegler, K., 2016. Argon, oxygen, and boron isotopic evidence documenting 40ArE accumulation in phengite during water-rich high-pressure subduction metasomatism of continental crust. Earth Planet. Sci. Lett. 446, 56–67.
Metrich, N., Joron, J.L., Berthier, B., 1998. Occurrence of boron-rich potassic melts in the Vulsini Volcanic District, Italy: evidence from melt inclusions. Geochim. Cosmochim. Acta 62 (3), 507–514. https://doi.org/10.1016/S0016-7037(97)00365-7.
Nakano, T., Nakamura, E., 2001. Boron isotope geochemistry of metasedimentary rocks and tourmalines in a subduction zone metamorphic suite. Phys. Earth Planet. Inter. 127 (1–4), 233–252.
Nikogosian, I.K., van Bergen, M.J., 2010. Heterogeneous mantle sources of potassium-rich magmas in central-southern Italy: melt inclusion evidence from Roccamonfina and Ernici (Mid Latina Valley). J. Volcanol. Geotherm. Res. https://doi.org/10.1016/j.jvolgeores.2010.06.014.
Nikogosian, I., Ersoy, Ö., Whitehouse, M., Mason, P.R.D., De Hoog, J.C.M., Wortel, R., van Bergen, M.J., 2016. Multiple subduction imprints in the mantle below Italy detected in a single lava flow. Earth Planet. Sci. Lett. 449, 12–19. https://doi.org/10.1016/j.epsl.2016.05.033.
Nikogosian, I., Bracco Gartner, A.J., Ersoy, Ö., Van Bergen, M.J., 2019. Heterogeneous deep source versus shallow crustal imprints in the petrogenesis of kamafugites from San Venanzo volcano, Italy. Acta Miner. -Petrogr. Abstract Ser. 10, 93, 93.
Palmer, M.R., Swihart, G.H., Grew, E.S., Anovitz, L.M., 1996. Boron: mineralogy, petrology and geochemistry. Rev. Mineral 33, 709–744.
Palmer, M.R., 2017. Boron cycling in subduction zones. Elements 13 (4), 237–242. https://doi.org/10.2138/gselements.13.4.237.
Palmer, M.R., Ersoy, E.Y., Akal, C., Uysal, I., Genç, S.C., Banks, L.A., Cooper, M.J., Milton, J.A., Zhao, K.D., 2019. A short, sharp pulse of potassium-rich volcanism during continental collision and subduction. Geology 47 (11), 1079–1082. https://doi.org/10.1130/G45836.1.
Peccerillo, A., 1999. Multiple mantle metasomatism in central-southern Italy: geochemical effects, timing and geodynamic implications. Geology 27 (4), 315–318.
Peccerillo, A., Panza, G.F., 1999. Upper mantle domains beneath central-southern Italy: petrological, geochemical and geophysical constraints. Pure Appl. Geophys. 156, 421–443.
Peccerillo, A. (2005). Plio-Quaternary Volcanism in Italy (Vol. 365). New York: Springer-Verlag Berlin Heidelberg.
Peccerillo, A., Frezzotti, M.L., 2015. Magmatism, mantle evolution and geodynamics at the converging plate margins of Italy. J. Geol. Soc. London 172 (4), 407–427.

Peccerillo, A. (2017). Advances in volcanology: cenozoic volcanism in the Tyrrhenian Sea Region (2nd Edition). Retrieved from http://www.springer.com/series/11157.
Plank, T., Langmuir, C.H., 1993. Tracing trace elements from sediment input to volcanic output at subduction zones. Nature 362 (6422), 739–743.
Plank, T., 2014. The Chemical Composition of Subducting Sediments. Elsevier.
Rio, S., Métrich, N., Mosbah, M., Massiot, P., 1995. Lithium, boron and beryllium in volcanic glasses and minerals studied by nuclear microprobe. Nucl. Inst. Methods Phys. Res. 100 (1), 141–148. https://doi.org/10.1016/0168-583X(95)00267-7. B.
Rosatelli, G., Wall, F., Stoppa, F., Brilli, M., 2010. Geochemical distinctions between igneous carbonate, calcite cements, and limestone xenoliths (Polino carbonatite, Italy): spatially resolved LAICPMS analyses. Contrib. Mineral. Petrol. 160 (5), 645–661. https://doi.org/10.1007/s00410-010-0499-x.
Rosenbaum, G., Gasparon, M., Lucente, F.P., Peccerillo, A., Miller, M.S., 2008. Kinematics of slab tear faults during subduction segmentation and implications for Italian magmatism. Tectonics 27 (2).
Rosner, M., Erzinger, J., Franz, G., Trumbull, R.B., 2003. Slab-derived boron isotope signatures in arc volcanic rocks from the Central Andes and evidence for boron isotope fractionation during progressive slab dehydration. Geochem. Geophys. Geosyst. 4 (8) https://doi.org/10.1029/2002GC000438.
Rudnick, R.L., Fountain, D.M., 1995. Nature and composition of the continental crust: a lower crustal perspective. Rev. Geophys. 33 (3), 267–309.
Schellart, W.P., 2010. Mount Etna-Iblean volcanism caused by rollback-induced upper mantle upwelling around the Ionian slab edge: an alternative to the plume model. Geology 38 (8), 691–694. https://doi.org/10.1130/G31037.1.
Schiavi, F., Kobayashi, K., Nakamura, E., Tiepolo, M., Vannucci, R., 2012. Trace element and Pb-B-Li isotope systematics of olivine-hosted melt inclusions: insights into source metasomatism beneath Stromboli (southern Italy). Contrib. Mineral. Petrol. 163 (6), 1011–1031. https://doi.org/10.1007/s00410-011-0713-5.
Schmidt, M.W., 1996. Experimental constraints on recycling of potassium from subducted oceanic crust. Science 272 (5270), 1927–1930.
Smith, H.J., Spivack, A.J., Staudigel, H., Hart, S.R., 1995. The boron isotopic composition of altered oceanic crust. Chem. Geol. 126 (2), 119–135. https://doi.org/10.1016/0009-2541(95)00113-6.
Spakman, W., Wortel, R., 2004. A tomographic view on western Mediterranean geodynamics. The TRANSMED atlas. The Mediterranean Region from Crust to Mantle. Springer, Berlin, Heidelberg, pp. 31–52.
Sugden, P.J., Savov, I.P., Agostini, S., Wilson, M., Halama, R., Meliksetian, K., 2020. Boron isotope insights into the origin of subduction signatures in continent-continent collision zone volcanism. Earth Planet. Sci. Lett. 538, 116207 https://doi.org/10.1016/j.epsl.2020.116207.
Thomsen, T.B., Schmidt, M.W., 2008. Melting of carbonated pelites at 2.5–5.0GPa, silicate–carbonatite liquid immiscibility, and potassium–carbon metasomatism of the mantle. Earth Planet. Sci. Lett. 267 (1–2), 17–31.
Tonarini, S., Leeman, W.P., Ferrara, G., 2001. Boron isotopic variations in lavas of the Aeolian volcanic arc, South Italy. J. Volcanol. Geotherm. Res. 110 (1–2), 155–170. https://doi.org/10.1016/S0377-0273(01)00203-7.
Tonarini, S., Leeman, W.P., Civetta, L., D'Antonio, M., Ferrara, G., Necco, A, 2004. B/Nb and δ^{11}B systematics in the Phlegrean Volcanic District. Italy. J. Volcanol. Geotherm. Res. https://doi.org/10.1016/S0377-0273(03)00394-9.
Tonarini, S., Leeman, W.P., Leat, P.T., 2011. Subduction erosion of forearc mantle wedge implicated in the genesis of the South Sandwich Island (SSI) arc: evidence from boron isotope systematics. Earth Planet. Sci. Lett. 301 (1–2), 275–284. https://doi.org/10.1016/j.epsl.2010.11.008.
Walowski, K.J., Kirstein, L.A., De Hoog, J.C.M., Elliott, T., Savov, I.P., Jones, R.E., EIMF, 2021. Boron recycling in the mantle: evidence from a global comparison of ocean island basalts. Geochim. Cosmochim. Acta 302, 83–100. https://doi.org/10.1016/j.gca.2021.03.017.
Wu, S., Yang, Y., Jochum, K.P., Romer, R.L., Glodny, J., Savov, I.P., Agostini, S., De Hoog, C.M.J., Peters, S.T.M., Kronz, A., Zhang, C., Bao, Z., Wang, X., Li, Y., Tang, G., Feng, L., Yu, H., Li, Z., Zhang, L., Lin, J., Zeng, Y., Xu, C., Wang, Y., Cui, Z., Deng, L., Xiao, J., Liu, Y., Xue, D., Zhang, D., Jia, L., Wang, H., Xu, L., Huang, C., Xie, L., Pack, A., Wörner, G., He, M., Li, C., Yuan, H., Huang, F., Li, Q., Yang, J., Li, X., Wu, F., 2021. Isotopic compositions (Li-B-Si-O-Mg-Sr-Nd-Hf-Pb) and $Fe^{2+}/\Sigma Fe$ ratios of three synthetic andesite glass reference materials (ARM-1, ARM-2, ARM-3). Geostand. Geoanal. Res. 45 (4), 719–745.
Xu, J., Zhang, G.B., Marschall, H.R., Walters, J.B., Liu, S.Q., Lü, Z., Zhang, L.F., Hu, H., Li, N., 2022. Boron isotopes of white mica and tourmaline in an ultra-high pressure metapelite from the western Tianshan, China: dehydration and metasomatism during exhumation of subducted ocean-floor sediments. Contrib. Mineral. Petrol. 177 (4), 46.